Int. J. Multiphase Flow Vol. 14, No. 3, pp. 287–303, 1988
Printed in Great Britain

0301-9322/88 $3.00 + 0.00
Pergamon Press/Elsevier

CENTRIFUGAL SCALING OF ISOTHERMAL GAS–LIQUID FLOW IN HORIZONTAL TUBES

J. J. M. GERAETS†
Laboratory for Aero- and Hydrodynamics, Delft University of Technology, Delft, The Netherlands

(*Received* 16 *March* 1987; *in revised form* 2 *December* 1987)

Abstract—For testing the similarity criteria of isothermal gas–liquid flow, the flow of air and a water–glycerine mixture in a 50 mm dia horizontal tube is compared with that of helium and water in a 5 mm dia tube rotating around a parallel vertical axis (the effective gravity is 113 times the natural gravity). The Reynolds number, Froude number, Weber number and gas–liquid density ratio are equal in both systems. The test facility, enabling two-phase measurements at centrifugal accelerations up to 1200 times natural gravity in pipe diameters up to 10 mm is described. The dimensionless pressure drops agree within 19% and the absolute differences of the void fraction are <0.03. Also the flow patterns are in good agreement. The influence of the individual dimensionless groups has been investigated experimentally and comparisons are presented with general pressure drop and void fraction correlations.

1. INTRODUCTION

The prediction of pressure drop, void fraction and flow pattern during the simultaneous flow of liquid and gas or vapour is necessary for economic design and optimization of operating conditions in the petroleum, power and chemical industry. The use of similarity criteria in two-phase flow assists in the comparison and generalization of data and provides a better understanding of how to deal with two-phase flow. While similarity criteria for flows of single-phase fluids have been well-established and modelling using these criteria has long been an accepted practice, such determination for two-phase mixtures has been hampered by conflicting and incomplete formulations of the basic equations. However, if only relatively simple two-phase flows are considered, i.e. isothermal flow without mass transfer, similarity criteria can be developed in a rigorous way from the governing equations and boundary conditions (Chesters 1975). In themselves the similarity criteria do not provide a relation for predicting pressure drop or flow pattern. However, once the relationship is found (analytically or from experimental data) for one system, the conditions of dynamic similarity require the same relationship to apply to all similar systems. Chesters (1977) showed that a considerable length scale down factor can only be realized if the gravitational force in the model is several hundred times earth gravity. The latter can be achieved by rotating the tube with the two-phase flow around a parallel vertical axis. The direction of the centrifugal force is normal to the tube axis, which restricts the method to horizontal or nearly horizontal flow.

A centrifuge facility has been built which enables unique measurements of pressure drop, void fraction and flow pattern in gas–liquid flows at gravities up to 1200 times natural gravity. For testing the similarity criteria the pressure drop, void fraction and flow pattern in a 50 mm stationary test section are compared with those measured in a 5 mm rotating test section. The system pressure, temperature and rotation rate are chosen in such a way that dimensionless groups can be varied relatively easy. Much attention is paid to the geometrical similarity of the two test sections. The test facilities and experiments are described in detail‡ by Geraets (1986).

2. SCALING OF ISOTHERMAL TWO-PHASE FLOW

2.1. Similarity criteria

Consider two systems with an isothermal two-phase flow of a gas and a liquid, having the same dimensionless initial and boundary conditions at all dimensionless times. For a horizontal tube,

†Present address: Oce Nederland B.V., P.O. Box 101, 5900 MA Venlo, The Netherlands.
‡Readers who are interested in details of the experimental results or test facility can obtain a copy of the Ph.D. Thesis from the author.

for instance, the two requirements imply that the systems must be geometrical similar and the same ratio of the gas and liquid volume flow rates must be applied. Besides equality of any imposed distributions of velocity and pressure and of the ratio of gas to liquid velocities, dynamic similarity of the two flows requires equality of the six dimensionless parameters (Chesters 1975):

$$\mathrm{Re} = \frac{\rho_L U L}{\mu_L} = \text{equal} \qquad \text{Reynolds number} \qquad [1]$$

$$\mathrm{We} = \frac{\rho_L U^2 L}{\sigma} = \text{equal} \qquad \text{Weber number} \qquad [2]$$

$$\mathrm{Fr} = \frac{U^2}{gL} = \text{equal} \qquad \text{Froude number} \qquad [3]$$

$$\mathrm{Eu} = \frac{p_{G,\mathrm{char}}}{\rho_L U^2} = \text{equal} \qquad \text{Euler number} \qquad [4]$$

$$\frac{\mu_G}{\mu_L} = \text{equal} \qquad \text{gas–liquid viscosity ratio} \qquad [5]$$

$$\frac{\rho_{G,\mathrm{char}}}{\rho_L} = \text{equal} \qquad \text{gas–liquid density ratio,} \qquad [6]$$

where p, ρ, μ, g and σ denote, respectively, pressure, density, dynamic viscosity, acceleration due to gravity and surface tension; L is a characteristic length, chosen to be the diameter of the tube; U is a characteristic velocity, chosen to be the superficial liquid velocity (=liquid volume flow divided by the cross-sectional area of the tube). The subscripts G and L denote gas and liquid and char refers to a characteristic spot in the flow (here a spot in the gas outlet of the separator is chosen).

The first five parameters arise from the conventional governing equations, the last one from the boundary conditions. Any one of the six parameters may of course be replaced by any combination of itself with the others. From the first three parameters (Reynolds, Weber and Froude) the scale factors for length L_2/L_1, velocity U_2/U_1 and viscosity $(\mu_L)_2/(\mu_L)_1$ can be derived (1 indicates the original flow, 2 the model flow):

$$\text{equal} \quad \frac{\mathrm{We}}{\mathrm{Fr}} = \frac{L^2 \rho_L g}{\sigma} \qquad \text{leads to} \qquad \frac{L_2}{L_1} = \frac{\left(\dfrac{\sigma}{\rho_L}\right)_2^{1/2}}{\left(\dfrac{\sigma}{\rho_L}\right)_1^{1/2}} \left(\frac{g_1}{g_2}\right)^{1/2}; \qquad [7]$$

$$\text{equal} \quad \mathrm{We} \times \mathrm{Fr} = \frac{U^4 \rho_L}{g\sigma} \qquad \text{leads to} \qquad \frac{U_2}{U_1} = \frac{\left(\dfrac{\sigma}{\rho_L}\right)_2^{1/2}}{\left(\dfrac{\sigma}{\rho_L}\right)_1^{1/2}} \left(\frac{L_1}{L_2}\right)^{1/2}; \qquad [8]$$

$$\text{equal} \quad \frac{\mathrm{Re}^4 \mathrm{Fr}}{\mathrm{We}^3} = \frac{\rho_L \sigma^3}{g \mu_L^4} = Q \qquad \text{leads to} \qquad \frac{(\mu_L)_2}{(\mu_L)_1} = \frac{(\rho_L \sigma)_2^{1/2}}{(\rho_L \sigma)_1^{1/2}} \left(\frac{L_2}{L_1}\right)^{1/2}; \qquad [9]$$

Q is the liquid-property number, so-called since for constant g it depends solely on the liquid properties. The remaining three requirements determine the scale factor for pressure, mean molecular weight and gas viscosity:

$$\text{equal} \quad \frac{p_{G,\mathrm{char}}}{\rho_L U^2} \quad \text{leads to} \quad \frac{(p_{G,\mathrm{char}})_2}{(p_{G,\mathrm{char}})_1} = \frac{(\sigma \rho_L)_2}{(\sigma \rho_L)_1} \frac{L_1}{L_2}; \qquad [10]$$

$$\text{equal} \quad \frac{\rho_{G,\mathrm{char}}}{\rho_L} \quad \text{leads to} \quad \frac{M_2}{M_1} = \frac{\left(\dfrac{T\rho_L}{\sigma}\right)_2}{\left(\dfrac{T\rho_L}{\sigma}\right)_1} \frac{L_2}{L_1}; \qquad [11]$$

and by means of [10] and the perfect gas law: $p_G/\rho_G = RT/M$ (R = gas constant, T = temperature, M = mean molecular weight, here the masses in kg/mol are used),

$$\text{equal} \quad \frac{\mu_G}{\mu_L} \quad \text{leads to} \quad \frac{(\mu_G)_2}{(\mu_G)_1} = \frac{(\mu_L)_2}{(\mu_L)_1}. \qquad [12]$$

2.2. Satisfaction of the criteria

For g constant only certain liquids can scale each other and the choice of the scalant liquid completely determines the length and velocity scale factors. If g is variable, as can be achieved with a rotating model, or if some of the parameters are unimportant, the situation becomes more flexible (Chesters 1977). If we assume that $(\sigma/\rho_L)^{1/2}$ of the model fluid and original fluid do not differ very much (for most liquids: $3 \times 10^{-3}\,\text{m}^{3/2}/\text{s} < (\sigma/\rho_L)^{1/2} < 9 \times 10^{-3}\,\text{m}^{3/2}/\text{s}$) then the length scale factor becomes $L_2/L_1 = (g_1/g_2)^{1/2}$. The consequences for the other scale factor are given below.

Equation [8] requires a velocity in the model which is about $(L_1/L_2)^{1/2}$ greater than in the original flow. According to [9], the model fluid should have a considerably lower dynamic viscosity—which presents no problems unless the viscosity of the original liquid is low ($< 10^{-3}\,\text{Pa}\cdot\text{s}$). The requirement [10] leads to a greater absolute pressure in the model and [11] indicates that the model gas should ideally have a much lower molecular weight than the original gas. This will often not be possible since a molecular weight < 2 is unattainable. In this event one of the two basic requirements $p_G/\rho_G U^2 = \text{equal}$ or $\rho_{G,\text{char}}/\rho_L = \text{equal}$ must be dropped. The present method is restricted in its applicability to approximately horizontal flows where both expansion and pressure waves will often be negligible, certainly with regard to their influence on the local flow pattern.

Equality of the density ratio takes account of the influences of gas inertial forces on the liquid flow, which largely determine the development of interfacial waves. If the modelling of compressibility is relinquished the pressure scaling requirement [10] disappears. The requirement of equal density ratio can now be satisfied by adapting the scale factor for absolute pressure. Equations [10] and [11] are then replaced by

$$\frac{(p_{G,\text{char}})_2}{(p_{G,\text{char}})_1} = \frac{\left(\frac{\rho_L T}{M}\right)_2}{\left(\frac{\rho_L T}{M}\right)_1} \qquad [13]$$

Finally, [12] requires a model gas with a much lower viscosity than the gas of the original system. Because of the relatively small variation of μ among gases ($10 \times 10^{-6} < \mu_G < 30 \times 10^{-6}\,\text{Pa}\cdot\text{s}$) and the limitations on the choice of gases imposed by [13], it will generally not be possible to satisfy this requirement. The influence of gas viscosity in many two-phase flows is very slight however.

2.3. Consequences of the use of rotation to increase gravity

For reasons of symmetry the axis of rotation is chosen to be vertical, parallel to the direction of natural gravitational acceleration. For the body force per unit mass of the fluid, $\mathbf{g}$, to be approximately constant over the flow concerned, this flow may only have appreciable extension in the direction parallel to the axis of rotation and not in the radial direction. This confines the method of scaling to approximately horizontal flows: $D/R \ll 1$, where D is the diameter of the tube and R is the perpendicular distance from the test section to the axis of rotation. From $D \approx 0.005$ m and $R \approx 0.5$ m the ratio D/R becomes 0.01, which might be small enough to neglect the variation of the gravity in the radial direction. The flow direction is chosen to be downwards in the direction of the natural gravity. In order to fulfil the requirement of geometrical similarity the original large-scale flow is subjected to the same downward inclination as the model flow.

Due to lateral velocity fluctuations, coriolis forces arise. The largest fluctuations are to be expected in the direction of the gravity and the coriolis forces are then directed normal to the main flow and gravity. In the worst-case situation (high flow rates with intermittent flow patterns) the coriolis forces can be up to 15% of the centrifugal force; the experimental results are suspect then. At the flow rates the coriolis forces are negligible.

2.4. Test conditions

It is desirable to use water in the rotating test section to prevent changing of the fluid properties by leakage of cooling water into the circuit. For the large-scale flow a mixture of water and glycerine at 20°C is used. The required viscosity of the mixture is calculated from [9]. The factor $(\sigma\rho_L)_1^{1/2}/(\sigma\rho_L)_2^{1/2}$ ranges from 1.00 to 1.06 for all possible mixtures of water and glycerine. Hence, to the first approximation: $(\mu_L)_1 \approx 1.03\,(\mu_L)_2(L_1/L_2)^{1/2} = 3.3 \times 10^{-3}$ Pa·s, which corresponds to a solution of 38% glycerine by wt. For calculations $L_1 = 49.8 \times 10^{-3}$ m and $L_2 = 4.89 \times 10^{-3}$ m are used. The effective gravitational acceleration in the model can be calculated from [7]: $g_2/g_1 = 113$, which requires a rotation rate of 460 rpm. By means of [8] the velocity scale factor becomes $U_2/U_1 = 3.33$. The frequency scale factor is $(U_2/L_2)/(U_1/L_1) = 33.8$. All processes in the model flow are a factor of 33.8 faster than those in the original flow. The ideal ratio of the molecular weight is 0.090 according to [11]. With helium ($M = 4 \times 10^{-3}$ kg/mol) in the model flow and carbon dioxide ($M = 44 \times 10^{-3}$ kg/mol) in the original flow this value would almost be obtained. However, because of the high flow rates in the 50 mm section it is preferable to use air ($M = 29 \times 10^{-3}$ kg/mol) instead of carbon dioxide. In this case $M_2/M_1 = 0.138$. The scale factor for the absolute pressure [14] becomes $(p_{G,char})_2/(p_{G,char})_1 = 6.61$. The ratio of the Euler number now is $Eu_2/Eu_1 = 0.66$. The absolute pressure in either the stationary test section or rotating test section can however be chosen freely. High pressure (2.95 MPa) is applied to the rotating test section so that high centrifugal accelerations are practicable. The system pressure must be always higher than the (hydrostatic) pressure drop $\rho_L\omega^2R^2/2$ in the radial part of the rotor (see figure 2), otherwise an undesirable under pressure in the liquid circuit arises. The last requirement of equal viscosity ratio [12] cannot be fulfilled. The dynamic viscosity of helium is about three times the ideal value. The scale factor for the pressure drop $\Delta p/\Delta L$, calculated from [4], is 103.

Summarizing. A two-phase flow of air–water/38% glycerine in a 50 mm dia pipe with a downward inclination of 1:113 and an absolute pressure of 0.44 MPa is scaled with a helium–water flow in a 5 mm dia tube at 2.95 MPa and a gravity of 113 times natural gravity. Of the six similarity parameters the Reynolds number, the Froude number, the Weber number and the density ratio are equal in both systems. The mismatch of the Euler number is 0.66 and that of the viscosity ratio 3.57.

3. THE TEST FACILITY FOR TWO-PHASE EXPERIMENTS AT INCREASED GRAVITY

3.1. The centrifuge facility

The main components of the centrifuge facility are (see figure 1):

—The rotor with the test section (placed parallel to the vertical shaft).
—The protection cylinder with bearings in the cover and bottom.
—The V-belt drive and flexible couplings
—The mechanical seals for having a leakage-free passage of the liquid and gas from the stationary part to the rotating part of the circuit.
—The slip rings for output of electrical signals.

The rotor with the test section is depicted in figures 2 and 3. For cost and manufacturing reasons the diameter of the rotor is limited to 1 m. The length is 2 m, so that a 10 mm dia test section with sufficient length/diameter ratio (200) can be used. In this investigation a 5 mm dia tube is applied and only half of the total length is therefore in use. The rotation speed can be varied continuously between 0 and 1400 rpm.

3.2. The rotating test circuit

The main components of the rotating circuit are shown in figure 3. From the seals liquid and gas flow upward in the central lines to the top of the rotor, where the circuit can be vented. After the radial section, where the pressure increases due to the hydrostatic pressure rise, the liquid flows downward in a 10 mm dia tube 1 m long. At the start of the 10 mm section the liquid velocity is raised with a venturi to prevent back-flow of gas at low flow rates. In the mixing section gas is

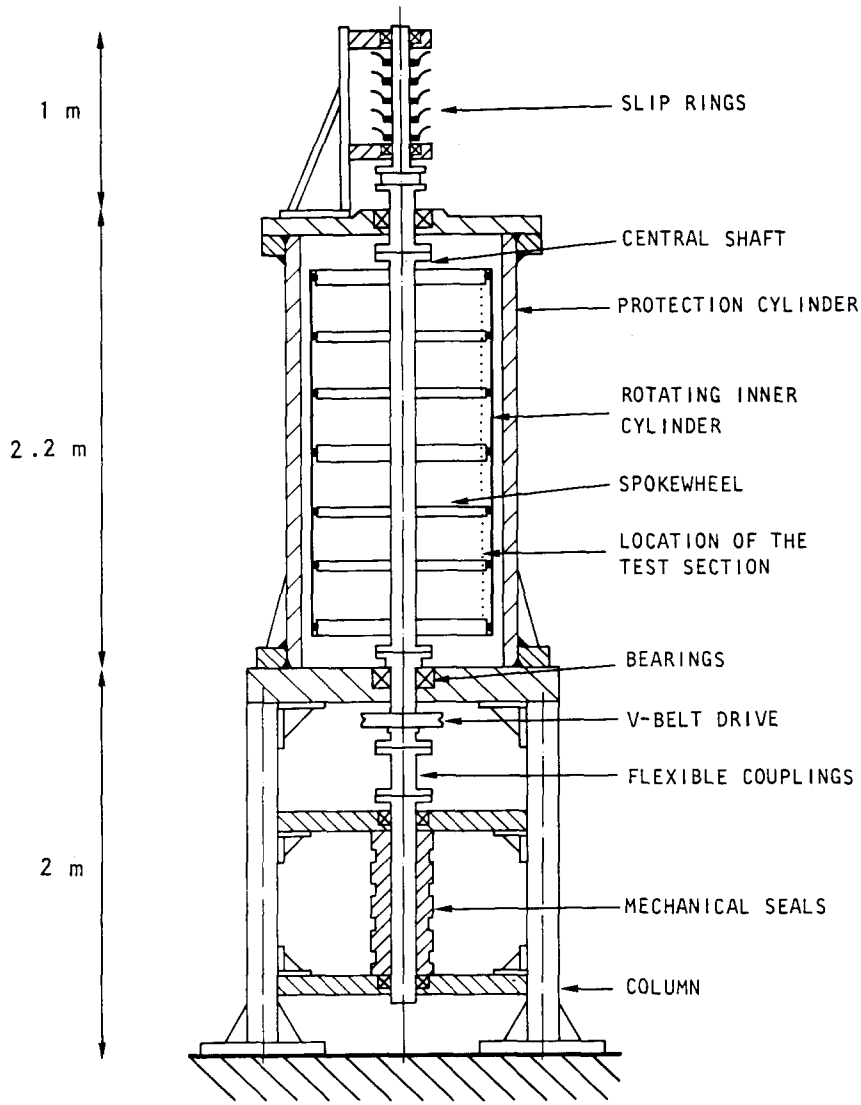

Figure 1. The centrifuge facility.

added to the liquid. No special demands are imposed on the geometry, only the similarity with the 50 mm test section is of interest.

The pressure is transmitted from the taps through liquid-filled lines to the pressure difference transducer which is mounted in the top of the shaft. Pressure differences ranging from 0.5 to 100 kPa can be measured with an accuracy of 2% of the measured value. Rotation of the transducer does not affect the sensitivity ($<0.1\%$), only a drift in the offset directly proportional to ω^2 occurs. The single-phase pressure drop is frequently checked during rotation and standstill. The difference between the measured value and the calculated value from the Blasius equation is always $<4\%$. For obtaining the frictional multiplier, ϕ_L^2, the total pressure drop is first corrected for the elevational pressure drop (with the help of the measured void fraction) and then divided by the calculated single-phase liquid pressure drop. Because of the low flow rates and the high operating pressure the pressure drop due to expansion can be ignored.

The entrance of the test section in the separator is chosen in such a way that with a half-filled separator the centre of the tube is 10 mm below the liquid level. In the ring-shaped separator (dia = 36 mm) liquid and gas flow in a circumferential direction. After a quarter of one revolution the liquid is extracted at the bottom of the tube close to the outerside of the ring and the gas at the top close to the inside of the ring, see figure 2. After the separator the fluids flow via the radial lines and the lines in the rotor shaft back to the seals.

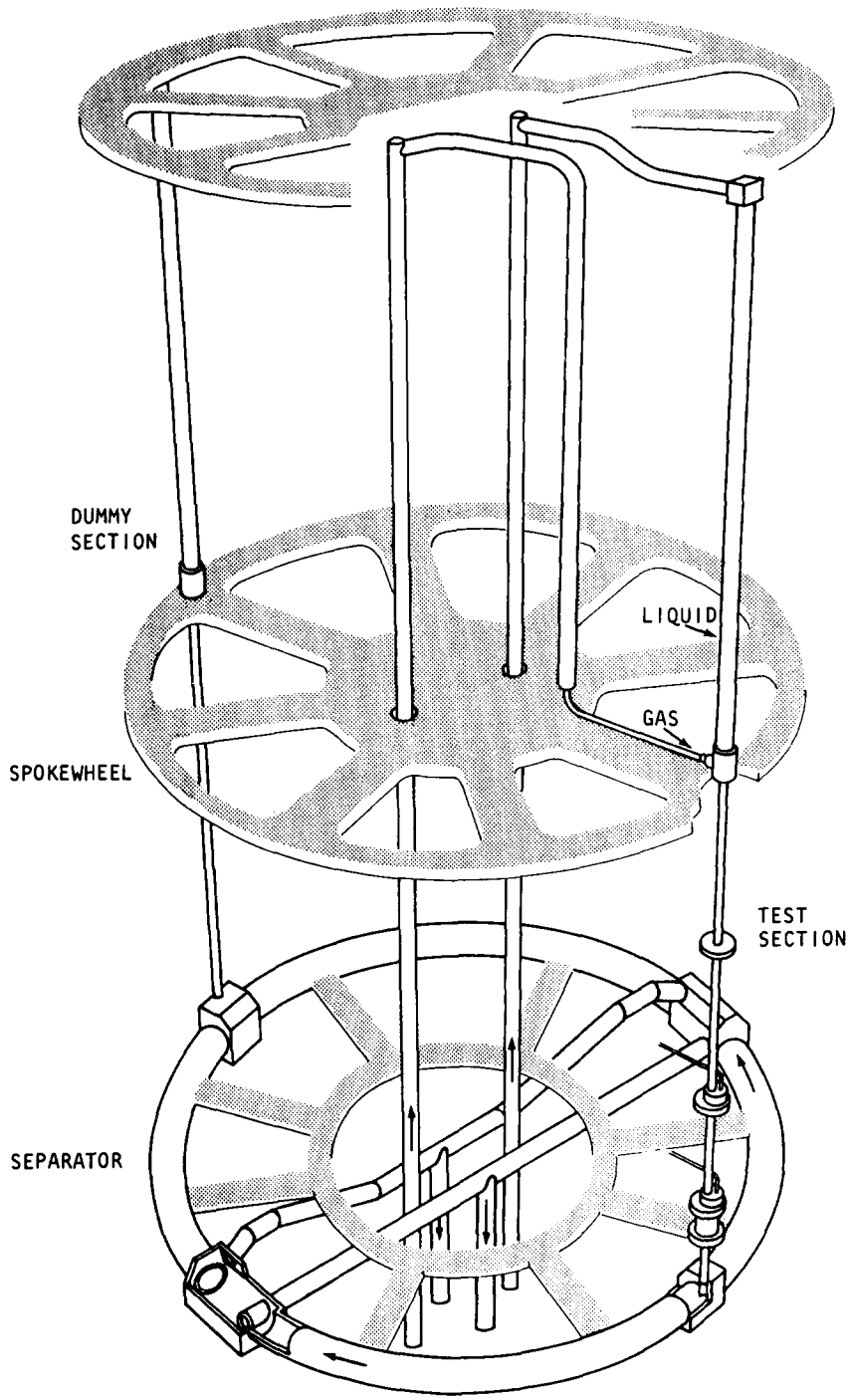

Figure 2. The rotor.

3.3. Measurement of the void fraction and the flow pattern

A new instrument has been developed for measuring void fractions in two-phase pipeflow. An extensive description of the void sensors is given in the accompanying paper (Geraets & Borst 1988) and by Geraets (1986). To allow accurate comparisons the same method is used in both the 5 and 50 mm test sections. The two sensors are geometrically similar and the calibration curves are very alike. The principle of the device is based on the measurement of the electrical capacitance of the two-phase mixture. The active length of the sensor is $2\pi D \approx 6$ dia. The electrode configuration consists of a helical cross capacitor by which spatial averaging is automatically realized. For

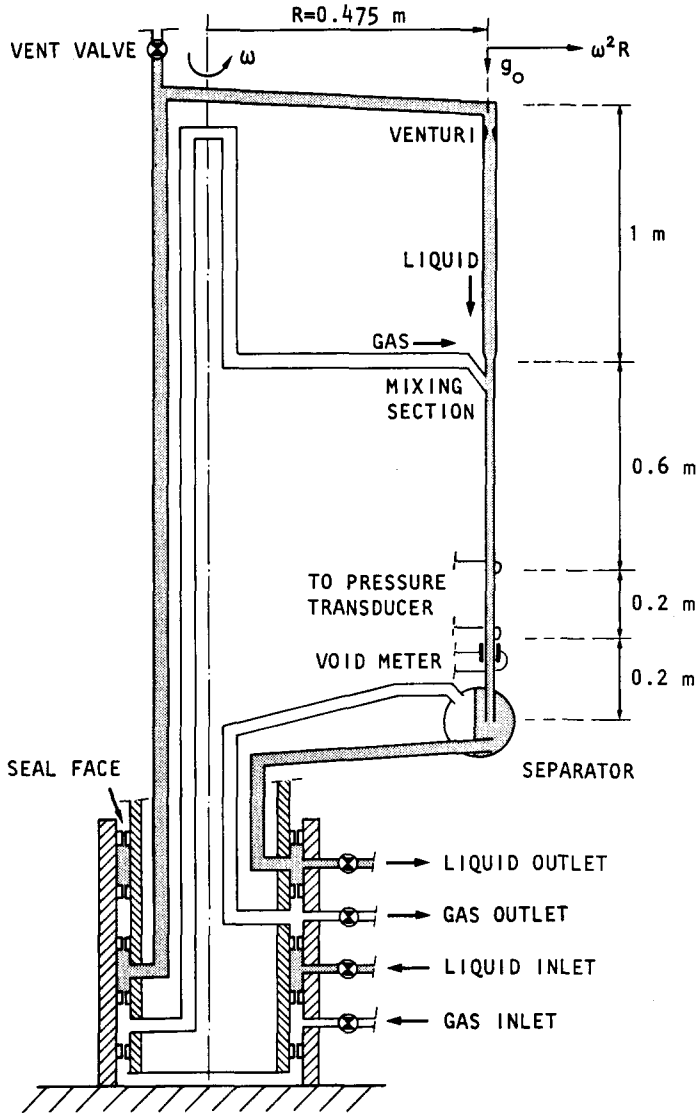

Figure 3. Diagram of the rotating loop.

comparing two flows the time-averaged value of the measured electrical capacitance is used for calculating the time-averaged void fraction $\bar{\alpha}$. In the experimental region of interest the maximum absolute error of the void fraction is ± 0.03 for stratified and intermittent flows (Geraets & Borst 1988).

The instantaneous output signal of the capacitance meter, which is a measure for the void fraction in the sensor volume, is used for flow pattern identification. The signal of the capacitance meter is recorded with a digital oscilloscope; the sample frequency being 0.2 kHz for the 50 mm sensor and 10 kHz for the 5 mm sensor. Because the calibration curves for the two geometrically similar sensors are almost equal, the time-varying output signal will be the same if the flow patterns are the same. Figure 7 shows some recorded signals. For stratified flow the distribution of the phases in a cross-sectional plane does not change with time and hence the void fraction is constant. In this study the flow is called plug (PL) if the sensor is completely filled during the passage of a "liquid wave" and the recorded void fluctuations look like a block signal. If the sensor is not completely filled during the passage of the "liquid wave" then the flow is called slug (SL) and the output signals resembles a sawtooth. If the output signal is alternating between a block and sawtooth signal then the flow is indicated by PS (plug or slug). The intermittent flow pattern are defined in this way solely for ease of comparison of the two flows. The semi-annular (SA) flow

pattern is characterized by a thick liquid layer on the bottom and a thin film at the top. The fluctuations in the void signal are caused by waves on the liquid surface and the passage of small frothy slugs. The slug and plug frequencies are determined simply by counting the peaks in the void signal. This is justified here because the frequencies are sufficiently low. The distance between two slugs is always larger than the axial extension of the sensor.

3.4. The liquid and gas circuit

Liquid is circulated by an eight-stage centrifugal pump at a maximum operating pressure of 4 MPa. Before the liquid enters the seal unit it is filtered and brought to the desired temperature with the help of a tubular heat exchanger.

A facility was built for blowing any gas or gas mixture through the test section at a maximum operating pressure of 4 MPa. The gas to be circulated is stored in a balloon (1.3 m^3) which is enclosed by a pressure vessel. By turning on the regulating valve, gas flows from the supply balloon via the seals and the rotating test section to a collecting balloon (3 m^3) which is enclosed by a pressure vessel. The pressure at the collecting balloon is kept constant by means of a large buffer vessel (capacity 70 m^3). With a full supply balloon the experiments can be run continuously for almost 2 h at a medium flow rate. The gas is pumped from the collecting balloon back to the supply balloon and the same amount of gas can be used several times. Before the gas flows into the test section it is filtered and if necessary heated by electric heating elements. After the test section the gas is dried and filtered. Temperature and pressure are measured in front of the flow meter and in the gas inlet and outlet. If helium or a helium–air mixture is used, the percentage of air is measured with a gas analyser.

The liquid and gas mass flow rates are measured with integral orifices. Needle valves, located downstream of the flow meters are used for regulating the flow rate. The flow meters are calibrated very conscienciously and checked frequently.

3.5. General procedure for measurements

The experiments are carried out in two periods each of about 3 weeks. Before and after a testing period the pressure difference transducer, the void sensor, the pressure gauges, the gas analyser and the flow meters are calibrated and the leakage of the rotating circuit is checked.

Before a two-phase flow is adjusted the pressure drop with liquid alone flowing through the test section is always measured and compared with the calculated value from the Blasius equation. The deviation is always $< \pm 4\%$. Then a two-phase flow is adjusted and for at least 30 s the averaged values (averaging time = 10 s) of the output signals of the differential pressure transducer, the void meter and the flow meters are measured. Three recordings are sufficient to obtain a reliable time-averaged value of the pressure drop and void fraction. The difference between two measurements is always $<3\%$ for the pressure drop and <0.01 for the void fraction. At the start and the end of the run, recordings are made of the rotation speed and the pressure and temperature in the gas outlet, liquid outlet and at the gas flow meter.

The experiments were repeated on different days and in different weeks. The reproducibility of the frictional multiplier is $\pm 5\%$ and that of the void fraction measurement is ± 0.02. In 12 out of 18 adjusted flows the reproducibility of the frictional multiplier is even better: $\pm 2\%$.

4. DESCRIPTION OF THE 50 mm TEST FACILITY

A sketch of the test section is given in figure 4. Much attention was paid to the geometrical similarity of the 50 and 5 mm test sections:

—The same length/diameter ratio (200) is used.
—The same inlet geometry is applied. The angle of the gas inlet to the direction of the main flow is 26°. The diameter of the gas inlet is $0.45D$ (D = dia test section).
—The same outlet condition is valid: the liquid level in the separator is always above the entrance of the test section in the separator.

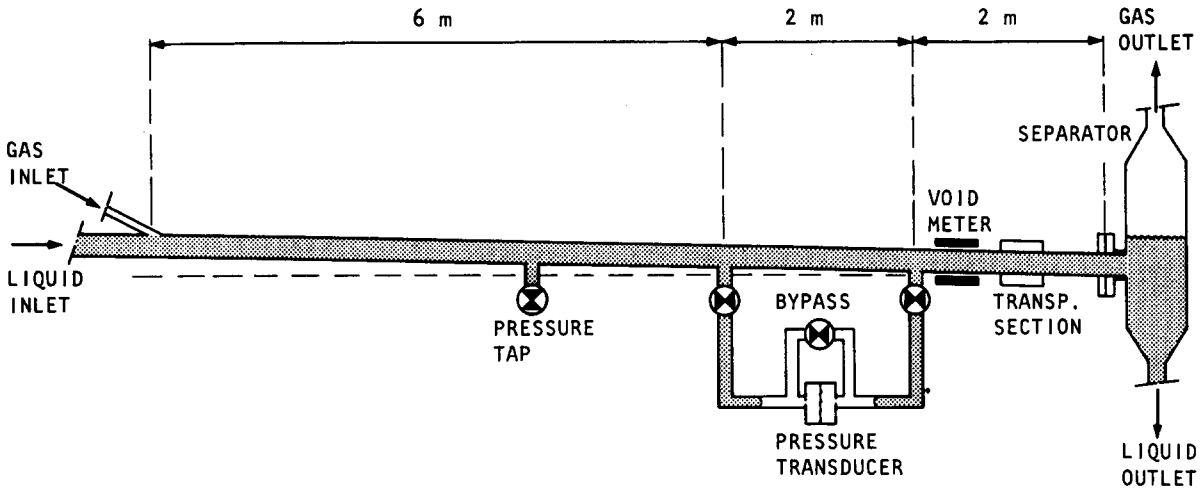

Figure 4. The 50 mm test section.

—The same dimensionless distance, $40D$, between the pressure taps is used.
—The same type of void sensor is applied

For the 50 mm test section the same equipment is used for circulating and conditioning the fluids as used for the 5 mm section.

4.1. Preliminary experiments

To fulfil the requirement of geometrical similarity the experiments are performed at a small downward inclination (1:113). By varying the effective gravitational acceleration in the rotating test section not only the Froude number is changed but also the inclination angle. To distinguish between the true Froude effect and the slope effect, the influence of the inclination of the tube on the pressure drop and flow pattern was first studied in the 50 mm section. Results from a horizontal test section are compared with those from the inclined section. It revealed that the pressure drop is only affected if the flow pattern is influenced and this only happens at low flow velocities (test conditions a_{11}, a_{12}, a_{21}, a_{22} and a_{31}, see table 1). At downward inclinations there is a preponderance of the stratified regime, which is in agreement with the results of Barnea *et al.* (1980).

5. EXPERIMENTAL RESULTS: CENTRIFUGAL SCALING

5.1. Ideal scaling

Eighteen test conditions (indicated by $a_{..}$) are examined, composed of four liquid velocities (the first subscript) and five gas velocities (the second subscript). Altogether 181 data are used and each test condition is adjusted at least 5 times. The results of experiments are given in table 1. Pressure drops, measured on different days and in different weeks agree within $\pm 5\%$, void fraction within ± 0.02 (absolute units).

As can be seen from figure 5 the agreement of the frictional pressure drop is very good. Only at two test conditions with low fluid velocities, a_{11} (▼) and a_{21} (■) is the difference $>20\%$. The closed symbols indicate a stratified flow pattern. If stratified flow situations are not considered, the largest deviations are $+5\%$ and -19%. The large differences at low fluid velocities with a stratified flow pattern are due to the specific construction details of the system, such as the entrance condition, the exit condition, vibrations of the system etc.

The time-averaged void fraction of the 5 and 50 mm tests differ <0.03 if stratified flow patterns (indicated by the closed symbols) are not considered, see table 1 and figure 6. At low fluid velocities back-flow of liquid from the separator is observed in the 50 mm test section. This may cause the observed deviations at stratified flow situations.

The flow pattern is deduced from the time-varying void signals in the manner described in subsection 3.3. Figure 7 shows some signals of the 50 and 5 mm sensors. Both the qualitative (flow

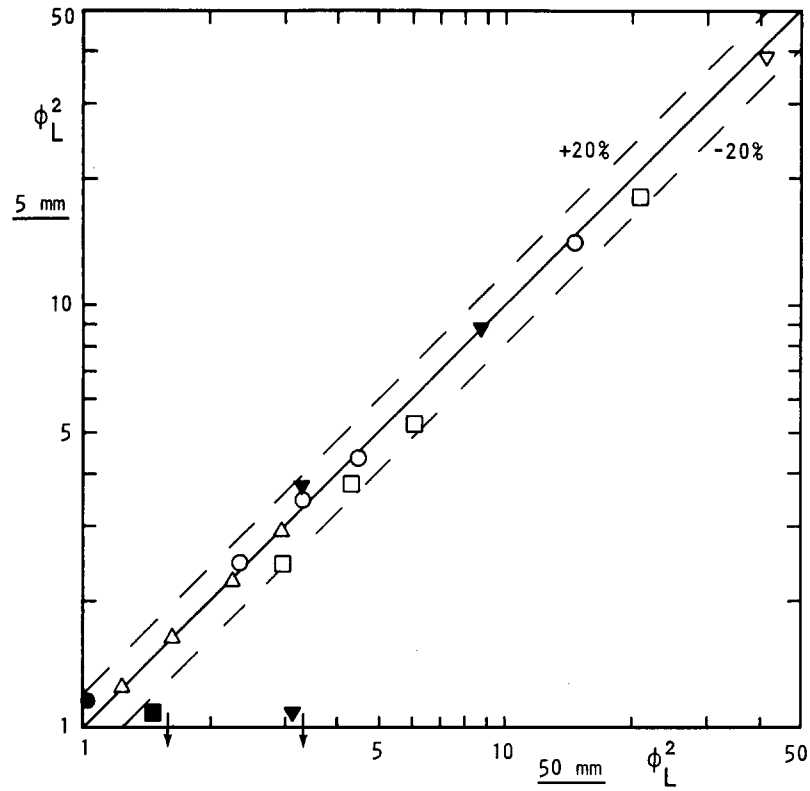

Figure 5. Comparison of the frictional multiplier; closed symbols indicate stratified flow.

pattern) and the quantitative (absolute values of the void fraction) agreement is very striking. Only in one case, which is close to a flow pattern transition [test condition a_{31} (●)], is the flow pattern different. By increasing the liquid velocity in the 50 mm section by only 10% plug flow is obtained. Possibly the transition in the rotating test section is triggered by vibrations of the system.

The plug and slug frequencies are determined simply by counting the peaks in the void signals. The reproducibility is $\pm 10\%$. Countings carried out by different persons produce the same result within 5%. The observations in the transparent 50 mm section differ $< 10\%$ from the countings

Table 1. Test conditions and experimental results of ideal scaling

Test condition	$(U_L)_{50}$	$(U_G)_{50}$	$(U_L)_5$	$(U_G)_5$	$(\phi_L^2)_{50}$	$(\phi_L^2)_5$	$(\bar{\alpha})_{50}$	$(\bar{\alpha})_5$	FP_{50}	FP_5
a_{11}	0.175	0.32	0.58	1.07	3.1	0.45	0.62	0.28	SS	SS
a_{12}	0.175	1.02	0.58	3.36	3.3	3.72	0.63	0.50	SS	SS
a_{14}	0.175	3.49	0.58	11.6	8.7	8.7	0.70	0.71	SW	SW
a_{15}	0.175	10.5	0.58	34.9	41.2	38.4	0.83	0.84	SA	SA
a_{21}	0.392	0.32	1.29	1.07	1.46	0.90	0.31	0.24	SS	SS
a_{22}	0.392	1.02	1.29	3.36	3.00	2.42	0.53	0.53	PL	PL
a_{23}	0.392	2.13	1.29	7.06	4.3	3.78	0.59	0.60	PS	PS
a_{24}	0.392	3.49	1.29	11.6	6.0	5.3	0.64	0.65	SL	SL
a_{25}	0.392	10.5	1.29	34.9	20.7	17.9	0.77	0.79	SA	SA
a_{31}	0.568	0.32	1.88	1.07	1.03	1.16	0.13	0.22	SS	PL
a_{32}	0.568	1.02	1.88	3.36	2.45	2.49	0.48	0.48	PL	PL
a_{33}	0.568	2.13	1.88	7.06	3.30	3.47	0.56	0.57	PS	PS
a_{34}	0.568	3.49	1.88	11.6	4.4	4.4	0.62	0.62	SL	SL
a_{35}	0.568	10.5	1.88	34.9	14.2	14.0	0.75	0.78	SA	SA
a_{41}	1.68	0.32	5.56	1.07	1.23	1.23	0.13	0.10	PL	PL
a_{42}	1.68	1.02	5.56	3.36	1.61	1.65	0.28	0.28	PL	PL
a_{43}	1.68	2.13	5.56	7.06	2.22	2.25	0.40	0.41	PL	PL
a_{44}	1.68	3.49	5.56	11.6	2.94	2.98	0.48	0.49	PS	PS

Symbols: a_{11}–a_{15}, ▽ or ▼; a_{21}–a_{25}, □ or ■; a_{31}–a_{35}, ○ or ●; a_{41}–a_{44}, △ or ▲. Flow pattern: SS = stratified smooth, SW = stratified wavy, SA = semi-annular, PL = plug, SL = slug, PS = plug or slug. ϕ_L^2 is the frictional multiplier, $\bar{\alpha}$ is the time-averaged void fraction.

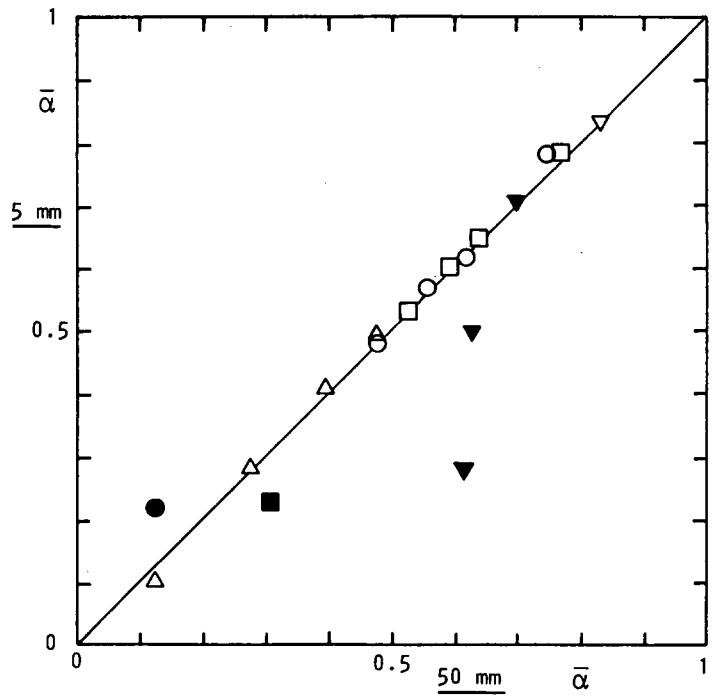

Figure 6. Comparison of the time-averaged void fraction; closed symbols indicate stratified flow.

of the void peaks. In table 2 the plug and slug frequency for the 5 and 50 mm test section and the ratio f_5/f_{50} are listed. The averaged value of the frequency ratio is 34.5 and the standard deviation is 3.2. The theoretical value of the frequency scale factor is $(U/L)_5/(U/L)_{50} = 33.8$ (!), see subsection 2.4. The plug frequency of the fluid velocity a_2 and a_3 increases with increasing gas velocity, whereas at the velocity a_4 the reverse occurs. This trend is predicted well by the model for slug frequency in horizontal pipes, developed by Taitel & Dukler (1977).

5.2. Comparison with the literature

Of the dozens of prediction methods for frictional pressure drop and void fraction published to date a few often cited correlations are discussed. Recently, Hewitt (1982) recommended the empirical Friedel (1979) and Chrisholm (1973) correlations for calculating frictional pressure drop. The region in which a particular correlation should be used was defined by means of the ratio of the liquid and gas viscosity and the dimensional total mass velocity $(\rho_L U_L + \rho_G U_G)$. The results of the scaling test show that these parameters cannot be used here. The viscosity ratio μ_G/μ_L and total mass velocity of the 5 mm test are, respectively, a factor of 3.6 and 3.0 larger than those in the 50 mm tests, whereas the frictional multiplier is the same. Because of the strong influence of the viscosity ratio in the Friedel correlation the predictions for the 5 mm tests are on average 20% higher than the predictions for the 50 mm tests. The dimensional Chrisholm correlation, applied to the present experiments, predicts values of the frictional multiplier which are in first approximation proportional to $(\mu_L/\mu_G)^{0.12}$ and inversely proportional to the square root of the mass velocity. The predicted values for the 5 mm tests are therefore half the values for the 50 mm tests.

Table 2. Plug and slug frequencies (s^{-1})

	a_{22}	a_{23}	a_{24}	a_{32}	a_{33}	a_{34}	a_{41}	a_{42}	a_{43}	a_{44}
f_5	11.5	14	24	21	19	29	92	93	61	60
f_{50}	0.35	0.45	0.68	0.52	0.50	0.82	2.95	2.57	1.93	1.82
$\frac{f_5}{f_{50}}$	32.8	31.1	35.1	40.6	38.0	35.5	31.2	36.2	31.6	33.0

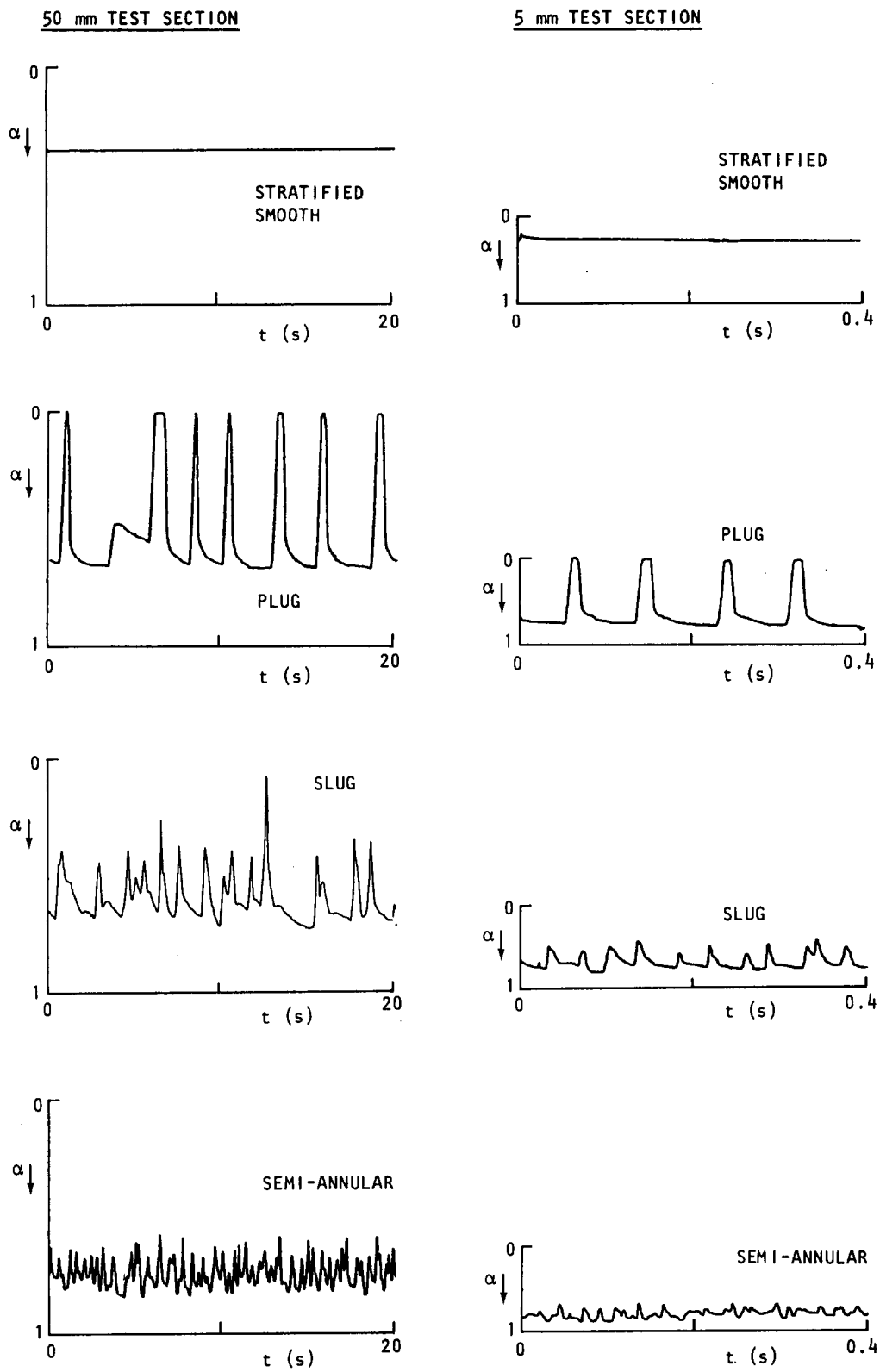

Figure 7. Time-varying void signals of the 50 and 5 mm tests, test conditions a_{21} (top), a_{22}, a_{24} and a_{25}. The scale of the vertical axis is not linear.

Measurements using water in the 50 mm test section do not differ significantly from the results with the water–glycerine mixture, see subsection 5.3.3.

Figure 8 shows a comparison of the frictional multiplier of the 50 mm tests and the predicted values from the Lockhart & Martinelli (1949) correlations, the Friedel (1979) correlation and the Dukler case I correlation (Dukler *et al.* 1964).

In table 3 the arithmetic-mean deviation

$$\bar{d} = \frac{1}{n}\sum_{i=1}^{n} d_i$$

and the standard deviation

$$\sigma = \left[\sum_{i=1}^{n} \frac{(d_i - \bar{d})^2}{n-1}\right]^{0.5}$$

are listed.

$$d_i = \frac{\left(\frac{\Delta p}{\Delta L}\right)_{\text{pred}} - \left(\frac{\Delta p}{\Delta L}\right)_{\text{meas}}}{\left(\frac{\Delta p}{\Delta L}\right)_{\text{meas}}}.$$

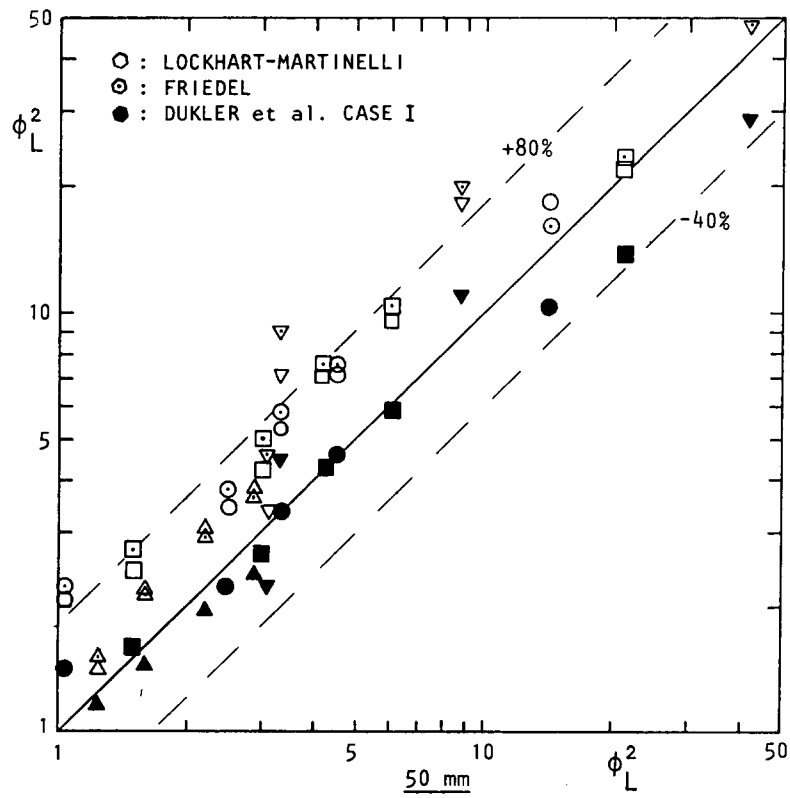

Figure 8. Comparison of the measured frictional multiplier of the 50 mm tests (horizontal axis) and the predicted value (vertical axis).

Table 3. Comparison of predicted pressure drop with the 50 mm tests

Prediction method	$\bar{d} \times 100\%$	$\sigma \times 100\%$
Lockhart–Martinelli	+52	32
Friedel	+61	43
Dukler case I	−6	21
Dukler case II	+23	24
5 mm tests, test conditions a_{11} and a_{21} are not considered	−2	9

The most simple correlation, Dukler case I, is seen to give the best predictions. The complicated Friedel correlation shows the largest differences with the 50 mm data. Moreover, the predictions of the Friedel correlation for the 5 mm test are 20% larger on average. The agreement of the 5 and 50 mm experimental data is much better than the predictions of any correlation. Note that only the Friedel correlation allows for influences of the Froude number or Weber number. In first approximation the frictional multiplier is proportional to $Fr^{-0.045}$ and $We^{-0.035}$.

The measured void fractions of the 50 mm tests are compared with the empirical correlation of Lockhart & Martinelli (1949) and the correlation of Spedding & Chen (1984). Except for test condition a_{11} the predicted values are always larger than the measured values. The arithmetic-mean deviation

$$\frac{1}{n}\sum_{i=1}^{n}\left[\frac{(\bar{\alpha}_{\text{pred},i}-\bar{\alpha}_{\text{meas},i})}{\bar{\alpha}_{\text{meas},i}}\right]=+0.04$$

for the Lockhart–Martinelli correlation and +0.06 for the Spedding–Chen correlation. The agreement of the 5 and 50 mm measurements (see figure 6) is much better than the predictions from the correlation, with the exception of stratified flow situations.

To predict flow pattern, frequently dimensional maps are used. Often the superficial velocities are used as co-ordinates and the maps depend strongly on the particular data being used to prepare them. In general, dimensional prediction methods must fail to predict the flow pattern for the original and model flow. Perhaps the most promising approach is that of Taitel & Dukler (1976). For horizontal and near horizontal flow the various transitions have been expressed in terms of dimensionless groups, essentially being U_G/U_L, Re, Fr, ρ_G/ρ_L and μ_G/μ_L in addition to the inclination angle. In view of the semi-theoretical base and the dimensionless form of the correlation, reasonable predictions are to be expected for a wide range of experimental conditions. The measured flow pattern and the influence of the inclination angle are predicted well by this method.

5.3. Variation of the dimensionless groups

Despite the mismatch of the gas viscosity, the viscosity in the 5 mm tube is actually too high, the agreement of the measurements in the 5 and 50 mm section is good. If the influence of the gas viscosity was important, then the frictional multiplier of the 5 mm tests should be higher than that of the 50 mm tests, whereas the reverse occurs.

5.3.1. Influence of the Euler number. Because the value of the Euler number Eu, defined here as $p_{G,\text{char}}/\rho_L U_L^2$, is high (100–10,000), the expansion of the gas is small over the distances of interest. Consequently, one may expect that the different value of the Euler number for the 5 and 50 mm tests ($Eu_5/Eu_{50}=0.66$) will not affect the results. The Euler number is lowered by a factor of 0.53 and 0.14 by lowering the gas pressure from 2.95 MPa to 1.55 and 0.40 MPa. In order to retain the same density of the gas, the molecular weight is raised by using air ($M_{air}/M_{He}=7.1$) and a helium/air mixture ($M_{mix}/M_{He}=1.8$) instead of helium. The frictional multipliers for the lower Euler cases differ <4% from the value of the ideal scaling situation. Hence as expected its influence is small. This result also indicates that acceleration effects are small.

5.3.2. Influence of the density ratio. For the rotating test section the effect of the density of the gas is tested by using air ($\rho_{air}/\rho_{He}=7.2$) instead of helium. A mixture of helium with 14% air by vol ($p_{mix}/p_{He}=1.8$) is also applied. The other dimensionless groups are preserved. In the 50 mm test section both the density ratio and the Euler number are lowered by a factor of 0.23 by decreasing the pressure from 0.44 MPa to atmospheric. In many two-phase flows the Euler number is not an important parameter so that the influence is principally that of the gas density. The other dimensionless groups remain unchanged. Only pressure drop and, for the 50 mm section, also flow pattern (from visual observations) are measured.

At low liquid flow rates the influence of the density ratio is considerable. At high liquid flow rates the effects are small. The trend is predicted well by the Dukler case I correlation (Dukler *et al.* 1964).

5.3.3. Influence of the Reynolds number. In the rotating system the Reynolds number is raised by a factor of 2 by decreasing the viscosity of the liquid. Of the remaining dimensionless groups the Weber number (+9%), the Euler number (+12%) and the viscosity ratio are affected. In the 50 mm test system the Reynolds number is raised by a factor of 3 by using water instead of a

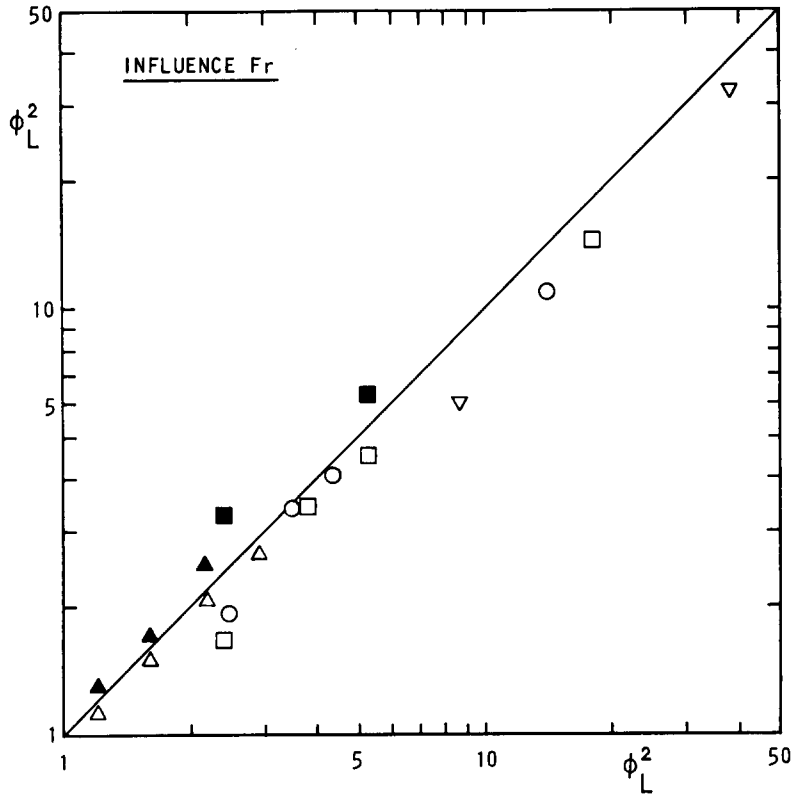

Figure 9. Influence of the Froude number; v = vertical axis, h = horizontal axis; Closed symbols, $Fr_v/Fr_h = 1.77$; open symbols, $Fr_v/Fr_h = 0.46$.

mixture of water and glycerine. Except for the Weber number (−11%) and the viscosity ratio the other dimensionless groups are preserved.

The frictional multiplier is hardly affected by the increase of the Reynolds number, the values are 4% larger on the average (test conditions with a stratified flow pattern are not taken into account). The difference between the void fraction is <0.01 for 29 of the 35 void fraction pairs. In one flow situation (condition a_{21}, 50 mm section) a flow pattern transition from stratified to plug is observed. The time-varying void signals show no larger differences than those observed with repeated measurements. The slug frequencies determined from the countings of the void peaks differ by <10%. Taking into account the large values of the Reynolds number it is not surprising that the actual value does not affect the void fraction and the flow pattern. Only a small layer at the wall is influenced.

5.3.4. Influence of the Froude number. In horizontal flow this number is an important parameter. The gravitational forces act on the liquid phase causing it to be displaced towards the bottom of the tube. Increasing the relative importance of gravity will lead to a better separation of the phases and probably lower pressure drops and lower void fractions. By increasing or decreasing the gravity the inclination angle is changed, as a result of which flow pattern transition can be provoked (this effect is only important at low flow velocities). The Froude number is varied by a factor of 0.46 ($g = 245\,g_0$) and 1.77 ($g = 65\,g_0$) with respect to the value required for ideal scaling, where g_0 is the acceleration due to the natural gravity. The other dimensionless groups are preserved.

In the high Froude number case, indicated by the closed symbols in figure 9, only pressure drop is measured. At the second (■) liquid velocity the pressure drop increases 25% on average. At the highest flow velocity (▲) the differences are small.

In the low Froude number situation the pressure drop is 15% lower on average and in five flow situations the void fraction is decreased by > 0.03. In these cases the largest reduction, about 30%, of the pressure drop is observed. In first approximation the pressure drop is proportional to $Fr^{0.3}$.

As can be seen from figure 10, where some noteworthy void signals are shown, the higher gravity results in a better separation of the phases. The plug frequency of the conditions a_{32} and a_{41} is lower,

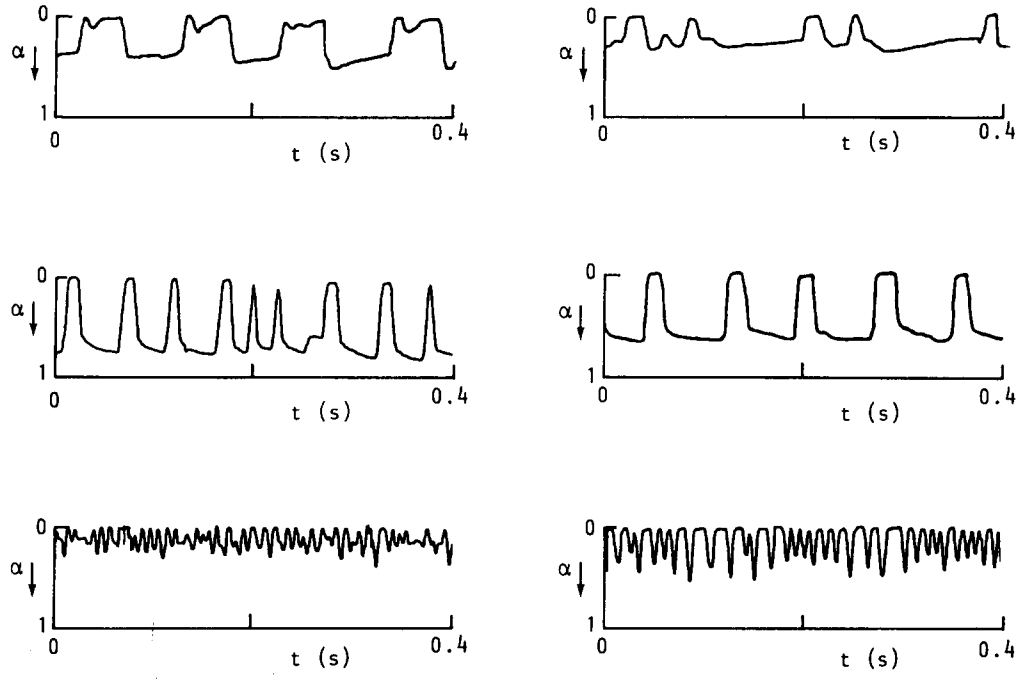

Figure 10. Influence of the Froude number on the time-varying void signal, test conditions a_{31} (top), a_{32} and a_{41}. The scale of the vertical axis is not linear. The right hand figures are for the low Froude number situation.

whereas the length of the liquid plug is larger. The small dip in the liquid plug of condition a_{31} (left-hand figure) seems to result in two separated small plugs in the right-hand figure. The change of intermittent flow in more stratified flow types can be described by the classical theory of Kelvin–Helmholtz instability. According to this theory higher gravities require higher gas velocities to obtain intermittent flow.

Only a very few prediction methods for two-phase pressure drop allow for influences of the Froude number, despite its great importance. Many correlations are of the homogeneous type or are deduced by graphic methods.

6. CONCLUSIONS

The agreement between the results of the original and centrifugal scaled flows is very good. Except for the conditions with a stratified flow pattern the frictional multiplier differs $<19\%$; at the two highest liquid velocities the difference is less even than 5%. The void fraction agrees within ± 0.03 with the exception again of the conditions with very low velocities. The time-varying void signals from which the flow pattern is deduced are similar in detail. Only in one case, is the flow pattern different.

Consequently, the six dimensionless groups, the ratio of the gas and liquid velocity and the geometry of the system completely determine the flow. These results emphasize that dimensionless groups have to be used for developing correlations or comparing measurements.

The variation of the effective gravity over the tube and the coriolis forces are of negligible influence, in the flow regimes concerned.

The viscosity ratio and Euler number, which are different for the original and model flow are of minor influences. The Froude number and gas-liquid density ratio are the most important parameters in the flow regimes studied. Lowering of the Foude number by a factor of 2 causes significant differences in pressure drop, void fraction and flow pattern.

Acknowledgements—The author wishes to acknowledge with gratitude the consistent guidance and encouragement of Professor G. Ooms. He also wishes to thank Professor A. K. Chesters for the inspirational

discussions. He is greatly indebted to the students and technical staff of the Delft University of Technology, in particular G.v.d. Velden, for making the rotating test facility a success.

REFERENCES

BARNEA, D., SHOHAM, O., TAITEL, Y. & DUKLER, A. E. 1980 Flow pattern transition for gas–liquid flow in horizontal and inclined pipes. *Int. J. Multiphase Flow* **6,** 217–225.

CHESTERS, A. K. 1975 The applicability of dynamic-similarity criteria to isothermal, liquid–gas, two-phase flows without mass transfer. *Int. J. Multiphase Flow* **2,** 191–212.

CHESTERS, A. K. 1977 A note on the centrifugal scaling of horizontal isothermal, liquid–gas flows without mass transfer. *Int. J. Multiphase Flow* **3,** 235–241.

CHRISHOLM, D. 1973 Pressure gradients due to friction during the flow of evaporating two-phase mixtures in smooth tubes and channels. *Int. J. Heat Mass Transfer* **16,** 347–358.

DUKLER, A. E., WICKS, M. & CLEVELAND, R. G. 1964 Frictional pressure drop in two-phase flow, B: An approach through similarity analysis. *AIChE Jl* **10,** 44–51.

FRIEDEL, L. 1979 Improved friction pressure drop correlation for horizontal and vertical two-phase pipe flow. Presented at *Eur. Two-phase Flow Group Mtg.*, Ispra, Italy, Paper E2.

GERAETS, J. J. M. 1986 Centrifugal scaling of isothermal gas–liquid flow in horizontal tubes. Ph.D. Thesis, Delft Univ. of Technology.

GERAETS, J. J. M. & BORST, J. C. 1988 A capacitance sensor for two-phase void fraction measurement and flow pattern identification. *Int. J. Multiphase Flow* **14,** 305–320.

HEWITT, G. F. 1982 Pressure drop. In *Handbook of Multiphase Systems*, Chap. 2.2 (Edited by HETSRONI, G.). McGraw-Hill, New York.

LOCKHART, R. W. & MARTINELLI, R. C. 1949 Proposed correlation of data for isothermal two-phase, two-component flow in pipes. *Chem. Engng Prog.* **45,** 39–48.

SPEDDING, P. L. & CHEN, J. J. J. 1984 Holdup in two-phase flow. *Int. J. Multiphase Flow* **10,** 307–339.

TAITEL, Y. & DUKLER, A. E. 1976 A model for predicting flow regime transitions in horizontal and near horizontal gas–liquid flow. *AIChE Jl* **22,** 47–55.

TAITEL, Y. & DUKLER, A. E. 1977 A model for slug frequency during gas–liquid flow in horizontal and near horizontal pipes. *Int. J. Multiphase Flow* **3,** 585–596.